Natural Resources for Human Health
eISSN: 2583-1194

Original Research

Received 22 May 2026
Revised 26 June 2026
Accepted 18 July 2026

Natural Resources for Human Health 2026, Vol. 6 (8s): 852–875

KEYWORDS:
Azithromycin; Electro-catalytic ozonation; Advanced oxidation processes; Cu–Fe/activated carbon; Hybrid electrochemical reactor; Antibiotic removal.

Synergistic Electro-Ozonation Degradation of Azithromycin in Wastewater using a Cu–Fe/Activated Carbon Catalyst: Experimental Investigation and RSM-Based Optimization

Muwafaq Kh. Sulaiman[1], Aysar T. Jarullah[1]

[1]Department of Chemical Engineering, College of Engineering, Tikrit University, Tikrit, Iraq.
Corresponding author:
Muwafaq Kh Sulaiman , Department of Chemical Engineering, College of Engineering, Tikrit University, Tikrit, Iraq
Email: mowafaq.khalaf@gmail.com

ABSTRACT: Antibiotic resistance has reached critical levels globally, largely due to improper antibiotic use the Objective of the study of this research was to high efficiently remove azithromycin from wastewater and its action mechanism by hybrid system. Azithromycin has been an antibiotics widely used in treating a variety of diseases, but it could be a pollutant on environment especially based on their persistence and the ability to create resistance. In this work, a novel cooperative electro-ozonation system with the catalyst of Cu(5%)–Fe(5%)/AC was developed for azithromycin (azithromycin) degradation during wastewater treatment. Tests were carried out with a bench electrochemical reactor comprising stainless steel anodes and carbon–poly(vinyl alcohol) (C-PVA) cathodic beds applied at low voltage (5 V), combined with flotation assisted by ozone. The effects of key operating parameters such as liquid flow rate, ozone flotation intensity O3 and solution pH in addition to temperature (25–50 °C) on azithromycin degradation were systematically investigated. Removal efficiency of electro-ozonation–Cu–Fe/AC process is far beyond that of ozonation alone, simply sole electrochemical oxidation (electricity, electricity method) and noncatalytic electro-ozonation, which obviously reflects many kinds of synergy roles by changing each other from anodic oxidation to ozone studying and heterogeneous catalysis. The degradation of azithromycin conformed to a pseudo-first-order equation, and the kinetic rates increased with temperature. The Response Surface Methodology (RSM) was adopted to be a complementary statistical tool for studying the combined effect of process variables and for optimizing performance. Statistical results showed that liquid flow rate and reaction time were essential factors affecting azithromycin conversion, in accordance with the experimental phenomena. The developed RSM model had a high predictive capability and reliability, suggesting its applicability for process optimization. Herein, the stabilities of Cu–Fe/AC catalyst are reliable in cycles reuse and stable under EZO conditions. The results suggest that aimed at degradation of azithromycin in wastewater, conversion can reach 100%, the high stability of,in azithromycin initial concentration 40ppm electro-ozonation–Cu–Fe/AC treatment concept is effective and is a promising technique for advanced treatment and provide guidance to design, and optimize hybrid-oxidation techniques treating pharmaceutical pollutants.

Natural Resources for Human Health
eISSN: 2583-1194

1. INTRODUCTION

The safety of drinking water and wastewater-treated water has attracted much attention due to the lack of water resources. However, human society is suffering from the adverse outcomes related to the contamination of aquatic systems deriving from domestic**,** agricultural and industrial activities[1].there for Antibiotic resistance is a global problem with significant medical risks and economic implications[2]. Earlier studies have linked high antibiotic use to increased prevalence of antibiotic-resistant bacteria threatened by pharmaceutical compounds being detected in samples from aqueous environment, such as river water, ground water and drinking water related to the effluent of wastewater treatment plants[3]**.** Antibiotics, as a main category of widely-used drugs to treat an extensive number of bacterial infections, can be detected in various water bodies as a result of their incomplete absorption during their metabolization and continuous use. It has been revealed that antibiotics can induce the selection of resistant bacterial strains in contact with living beings that would cause diseases untreatable with antibiotics and decreasing the ability to stop epidemics[4][5].The residues of antibiotics in aquatic system caused environmental and public heath, because of their broad use, long persistence and potential induction of microbial resistance even at trace level. One of them, azithromycin (azithromycin) – a highly utilized macrolide antibiotic – frequently can be detected in waste waters, surface water and even in drinking water due to the fact that it was removed just partially at the conventional plants of treatment [6]. Hospitals, pharmaceutical industry discharges, agriculture, aquaculture and domestic wastewaters are the main routes of azithromycin contamination of the environment (concentrations reported globally in the range ng L^{-1}–μg L^{-1} (exceeding suggested safe limits on some occasions)) [7] .The recalcitrant nature of azithromycin and other new contaminants, as well as their persistence in time, and the possible effects on the ecosystem , mark the need for alternative technologies to biological and physical treatments that have been most used but not always have led to full removal of such pollutants [6].The AOPs (Advanced oxidation processes) such as chemical precipitation, oxidation coagulation and adsorption have been increasingly engaged for the removal of refractory organic pollutants because they generated powerful oxidizing specie like hydroxyl radicals (•OH), these radicals can non-selectively perform oxidation of complex molecules [8]. Ozonation and electrochemical oxidation are the most applied AOPs in wastewater treatment. Ozonation: Ozonation is based on the high oxidizing capability of ozone (O_3) and was demonstrated to enhance degradation of pharmaceuticals and other emerging contaminants, although its efficiency can be hindered by mass transfer limitations but also by a sub-optimal mineralization of organic matter when applied alone [9]. On the other hand, because it is a green process of in sit generating oxidants for both degradations of organics pollutant, electro-oxidation is believed to be sustainable without adding chemicals on electrode surfaces and it fits in with treatment of refractory organic pollutants [10]. To increase treatment efficiency and make up for the shortcomings in these processes, a concept of hybrid oxidation systems developed by coupling two or more alternative system (such as electro-ozonation) has also been extensively studied. OZEO(ozone electro oxidation) is an application of ozone addition in electrochemical cell for enhancement of transport properties and reactive species production giving beneficial degradation kinetics and treatment performance [11]. The electrochemical oxidation coupled with ozonation played a complementally function, which facilitated the ozone degradation into radicals to speed up the following reactions and produced a more reagent species for consumption, so that these obtained high-efficiency degradation performance of refractory organics. Addition step of anatase is for improving performance in the oxidation; at least this step can be achieved better by adding to the heterogeneous catalysts To oxidants, additional improvement effectiveness it added in ozone generation can be activated, and enhance reactive species. B. Bristow, G.A. Moore / Science of the Total Environment 610–611 (2018) 1539–1551 Values as high as \300 gH2O/kg Cads have been demonstrated for C-based catalysts — activated C; bio char and engineered carbon materials in ozone application system possessing high surface area, porosity; and capacity to promote re- active oxygen species generation plus the ability to adsorb K+ [12]. Loading transition metals (e.g., Fe, Cu) on carbon-based materials is a novel way to open up Fenton-like reaction, enhance electron transport toward promoting the degradation process and improve operation range flexibility[13]. In previous work concerning the photo catalytic zonation system, the Fe-doped catalyst further accelerated azithromycin reduction by both direct •OH and hole-mediated pathways[14].Many attempts have been made by different research groups to remove azithromycin Camilo C. Castro-Jime´nezID1 , Julio C. Saldarriaga-Mol in last study get the removal is resulted in a significant AZT removal efficiency of 65% in distilled water after 60 min of treatment. In synthetic wastewater, the rate of AZT removal increased to 80%, in comparison, in a real effluent of a municipal wastewater treatment plant, an AZT removal of 56% wasobtained [15]. the in-depth research on the utilization of continuous-flow electro-zonation and interplay with heterogeneous catalysis for convenient antibiotic pollutants removal such as azithromycin is still vacant due to much less

literature except that some AOPs or hybrid oxidation methods have largely been developed within these years. Also, under a statistically optimized regime, the influence of the operational parameters (flow behavior, pH and temperature) to the purpose performance has not been well understood. From this perspective, the RSM is used as a statistical optimization tool to estimate and quantify interactions between multiple factors on one hand as its potentiality for design optimization through much less experimental runs [11]. we prepared the new reactor Cu(5%)–Fe(5%)/AC for zonation coupling electro catalysis system (O/EC) to degrade utilizing azithromycin (azithromycin), a first-line antibiotics residue in wastewater degradation. To unveil the impact of liquid flow rates, flotation strength and pH as well as temperature (25–50 °C) upon the process of OF using ozone, a lab-scale reactor containing pre-defined particles was used to treat OMEMSV. The RSM was employed as a secondary statistical model to aid in interpretation of the experiments as well as optimize performance of the process. It is anticipated that the integrated experimental–statistical method will be able to provide design and operational guidance in electra-ozonating advance treatment of antibiotic contaminated water .The specific objectives of this study were:(i) to evaluate the removal efficiency of azithromycin using the electro-catalytic zonation process,(ii) to investigate the synergistic interaction between electric current, ozone activation, and Cu–Fe catalytic sites,(iii) to model and optimize the operational parameters using Response Surface Methodology (RSM),(iv) to analyze degradation kinetics, and(v) to identify the dominant reactive oxygen species responsible for pollutant degradation.

2. MATERIALS AND METHODOLOGY

2.1 Chemicals and Reagents

Azithromycin (AZM)(C38H72N2O12) (samara factory) 99.9% was selected as the target pharmaceutical contaminant Activated carbon(AC) (CDH company) hydrated copper acetate (Cu2(CH3COO)4) , hydrated ferrous acetate (Fe(CH3CO2)2) (iSuoChem)and Polyvinyl alcohol (PVA) (iSuoChem) Working solutions with an initial concentration of 40 mg/L were obtained by diluting the stock solution with wastewater (or deionized water when specified). Methanol (sd fine chem limited) Potassium hydroxide (KOH)(BASFE company) was used as the supporting electrolyte. Sodium thiosulfate was used to quench residual ozone during sample collection.

2.2 Preparation of Cu–Fe/AC catalyst

A bimetallic Cu(5%)–Fe(5%)/activated carbon (Cu–Fe/AC) catalyst was synthesized using a impregnation method. Activated carbon was initially washed with deionized water and dried. Aqueous solutions of copper and iron precursors were prepared to achieve target metal loadings of 5 wt% Cu and 5 wt% Fe.The activated carbon was impregnated with the mixed metal solution under continuous stirring, and dried at 100 °C for 24 h and calcination 2.5 hr at 850 ° C under nitrogen figure (1) steps the preparation of catalyst

1- Mixing the hydrated copper acetate and hydrated ferrous acetate with di ionized water and stirring for 10 min

2- Adding AC on mixing in mixture hydrated copper acetate and hydrated ferrous acetate with di ionized water

3- Place the entire mixture in the ultrasonic mixer at 60 C° and 50 frequency for 1 hour .

4- The mixture was transferred to a starring and heater, and blended and circulated using a temperature of 90 C° .

5- Draying the sample by box furnace at 100 C° in 24 hr.

6- Convert the sample of catalyst to tubular furnace after nitrogen purge for Calcination at 850 C° 2hr

7- Sample weight 49 gm. after calcination

8- Preparation of PVA. 100 ml of deionized water with 8 gm PVA at 75 C° for 80 min

9-Mixing 2 gm catalyst (cu+fe /AC) to 2 ml form PVA became past catalyst and place in furnace at 80 C° for 24 hr.

Natural Resources for Human Health
eISSN: 2583-1194

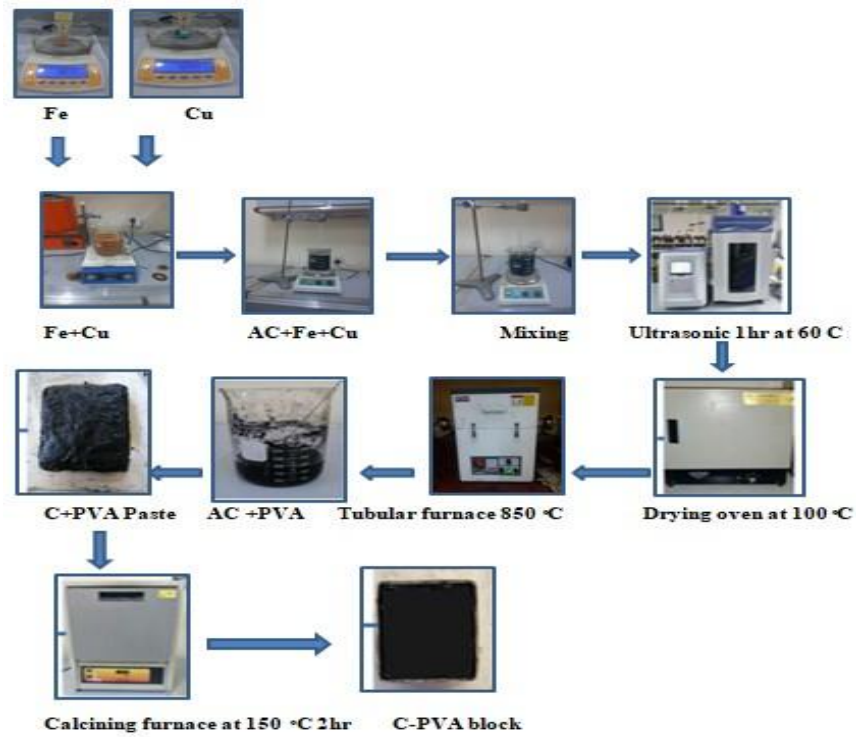

Figure (1): preparation of catalyst

2.3 Electro-ozonation reactor setup

The electro-zonation experiments were carried out into a continuous-flow bench-scale reactor (reactor dimensions: 40 × 110 × 120 mm; geometric volume = 0.528 L) with two stainless steel plates as the anodes (active area = 42 cm^2 each, rectangular shape: 70 × 60 mm) and two packed beds of carbon–poly(vinyl alcohol) blocks as cathode. Anode and cathode distance was kept 40 mm. Power supply was used to apply constant 5 V voltage and the operating current between 1 and 5 A, depends on the operation conditions. The addition, flotation and mixing of ozone (100% purity) were carried out by introducing the feed gas into the reactor with a flow rate of 8 L/min through a gas diffuser. **Figure (1)** No mechanical stirring was employed, mixing is by gassing. The Cu–Fe/AC catalyst was enclosed in a mesh and the dosage of the catalyst was 40 g for one time experiment. The electro-ozone experiments were conducted in a continuous-flow experimental reactor (reactor dimensions: 40 × 110 × 120 mm; geometric volume = 0.528 L) using two stainless steel plates as positive electrodes (effective area = 42 cm^2 each, rectangular shape: 70 × 60 mm) and two packed layers of carbon-polyvinyl alcohol blocks as negative electrodes. The distance between the positive and negative electrodes was maintained at 40 mm. A power supply was used to apply a constant voltage of 5 V, and the operating current ranged between 1 and 5 A, depending on the operating conditions. Ozone (100% purity) was added, floated, and mixed by introducing the feed gas into the reactor at a flow rate of 8 L/min via a gas distributor (Figure 2,3). No mechanical agitation was used; mixing was achieved by gasification. The Cu–Fe/AC catalyst was prepared with azithromycin by dissolving it in methanol. This catalyst was then added to water samples containing the same pollutant at various concentrations: 10, 15, 20, 25, 30, and 40 ppm. The system was then run for flushing with ionized water. An ozone generator was also started at a flow rate of 8 L/min at 100% concentration, and 0.2 M potassium hydroxide solution was added as the electrolyte. The power supply was then calibrated to 5 V. After start up, samples were taken every 10, 20, 30, and 40 minutes. A test sample was taken at each time point at a different flow rate (100, 150, 200, and 250 mL/min) until the optimal flow rate for the system was reached. The system was then flushed again with ionized water in preparation for the second concentration. The catalyst dosage was 40 grams per experiment.

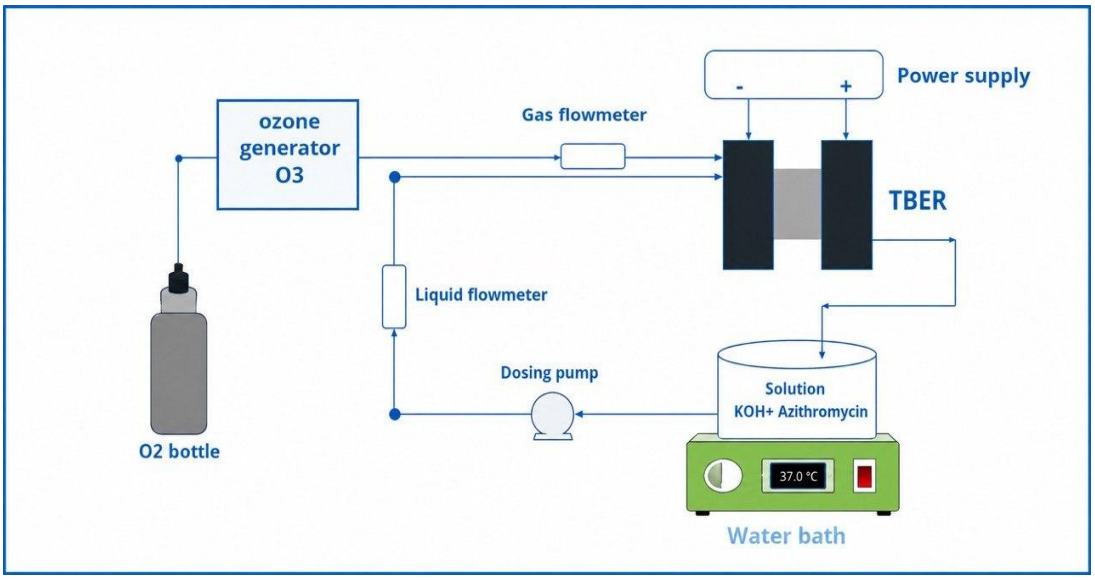

Figure (3) : Schematic diagram

2.4. *Experimental Design and Analysis of Variance (ANOVA)*

An experimental design is a set of runs such that the input parameters of a given configuration are changed to observe the behavior of the output response. Experiments are used to test the performance of systems and processes in any field[16] In this work, the optimal parameters for the ODS process may be obtained using the Central Composite Design (CCD) under the auspicious of Response surface methodology (RSM). RSM is a statistical and mathematical method to develop experimental models[17] I Cal approaches for building experimental models [16]. The benefit of the RSM vs. the usual full-factorial trial design is its cost feasibility while still incorporating interaction variables[18] . In addition, the RSM promises to reduce the numerical noise of conventional ones, by enabling the implementation of a derivative-based technique[19] Experimental data were fitted to two major equation models commonly employed in RSM for ODS about the coded values.the first –degree equation is:

$$yi = b + \sum bi\text{xi} + \varepsilon$$

And the second –degree equation

$$yi = b + \sum bi\ \ xi + \sum biixi^2 + \sum bijxixj + \varepsilon$$

where Y is the answer; xi and xj are the variables; b is the constant coefficient; bi, bj and bij are the interaction coefficients of linear, quadratic and second-order terms, respectively and ε is the modeling error The goal of experimental design is to determine the parameters that are most influential to the response, to verify where to locate the effective, controllable parameters for the response to be near the preferred optimal value, hence yielding low variability in the response and to reduce the influence of uncontrollable parameters. The RSM regression analysis is performed using the Experimental design tool (Design Expert 13). Design of experiments (DOE) was conducted using Design-Expert. It provides optimization, design with adjustable parameters, combination design and mixture design.[20] It is important to analyses the model once it is developed.[19] The variance can be analyzed in depth by means of a so-called analysis of variance (ANOVA) table. An ANOVA table can be used to: (i) determine whether a model is significant; for this purpose, it needs to perform regression plots and residual plots, (ii) check on its lack of fit, which is examined by comparing Fobs to the F-value, and (iii) analyses the model via R2 values, the greater the value of R2, the better the model's ability to describe experimental data.

2.5 Sampling and analytical methods

The outlet samples of the liquid phase were withdrawn from the reactor at predetermined time or steady-state intervals. Ongoing oxidations were quenched by addition of KOH immediately to wipe off any residual ozone. The filtered samples were subsequently filtered through 0.45 µm membrane filters. Analysis of azithromycin concentration was performed by UV–

Vis spectrophotometry at 212 nm (the formula used to calculate the % entrapment efficiency) according to calibration curve that was established within a linear range from 2 to 60 mg/L with an $R^2 = 0.9928$. The efficiency of removal was calculated using the formula

$$\text{Removal}(\%) = \left(\frac{(C0-C)}{C0}\right) * 100$$

where (C0)and (C) are the initial and residual AZM concentrations, respectively.

3. RESULTS AND DISCUSSION

3.1 Catalyst stability and operational robustness

The Cu–Fe/AC catalyst demonstrated good stability over six consecutive treatment cycles, with only a slight decline in AZM removal efficiency. The maintained performance indicates strong metal–support interactions and effective catalyst immobilization. Comparable stability has been reported for carbon-supported bimetallic catalysts in advanced oxidation systems [13]

3.2Structural Studies

The prepared catalyst was characterized using AFM , XRD,FTIR, and BET surface area analysis BET ,TGA ,SEM to evaluate surface morphology Figure (1), elemental distribution, crystalline structure, and textural properties

3.2.1 AFM

Atomic force microscopy (AFM) Figure (3) was employed to investigate the surface morphology and topographic characteristics of the prepared Cu–Fe/activated carbon catalyst. The two-dimensional and three-dimensional AFM images revealed a highly heterogeneous surface composed of densely distributed Nano scale protrusions and irregular nodular structures. The catalyst surface showed significant roughness compared to typical smooth carbon surfaces, indicating that the impregnation process successfully modified the activated carbon texture. The 3D topographic images demonstrated the formation of numerous Nano-sized peaks uniformly distributed over the catalyst surface. These peaks correspond to deposited Cu and Fe oxide clusters anchored onto the activated carbon matrix. The absence of large agglomerated domains suggests good dispersion of the metal species and effective anchoring on the support surface. Such homogeneous distribution is essential in catalytic ozonation systems because ozone activation occurs on exposed surface active sites. Particle size analysis confirmed that the majority of surface features were in the nanometer range, with a broad but continuous size distribution and a large number of small particles dominating the surface coverage. The high density of nano-features significantly increases the available surface area and creates additional catalytic active centers. Consequently, more adsorption sites become available for azithromycin molecules, improving their accessibility to reactive oxygen species generated during the electro-ozonation process. Furthermore, the increased surface roughness enhances mass transfer at the solid–liquid interface by reducing diffusion limitations near the catalyst surface. The irregular topography also facilitates ozone decomposition on the catalyst surface, promoting the formation of hydroxyl radicals and other reactive oxygen species. Therefore, the AFM results provide direct physical evidence supporting the observed improvement in azithromycin degradation efficiency. Overall, the AFM characterization demonstrates that the UV-assisted impregnation method successfully produced a nanostructured catalytic surface with high roughness and well-dispersed metal sites. The enhanced surface morphology plays a key role in accelerating oxidation reactions and contributes to the synergistic performance of the electro-ozonation system.

Natural Resources for Human Health
eISSN: 2583-1194

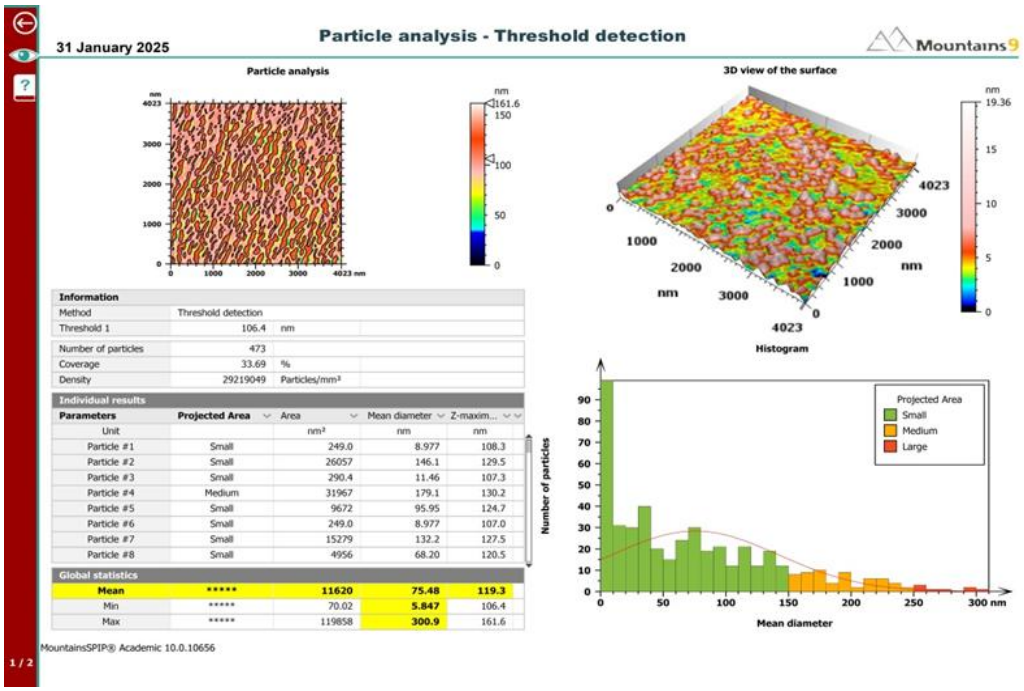

Figure (3): Atomic force microscopy

3.2.2 XRD

X-ray diffraction (XRD) **Figure (4)** analysis was performed to identify the crystalline phases present in the synthesized Cu–Fe/activated carbon catalyst and to verify the successful incorporation of metal species onto the activated carbon support. The diffraction pattern shows a broad peak centered around 2θ ≈ 23–26°, which is characteristic of amorphous carbon. This broad hump corresponds to the (002) plane of graphitic carbon and confirms that the activated carbon support possesses a predominantly amorphous structure with low crystallinity. In addition to the carbon peak, several distinct diffraction peaks were observed at approximately 2θ ≈ 43°, 50°, and 74°. These reflections are attributed to crystalline copper species, likely corresponding to CuO/Cu_2O phases deposited on the carbon surface. The sharpness and intensity of these peaks indicate the formation of well-defined copper oxide crystallites anchored on the activated carbon matrix. Furthermore, secondary diffraction peaks appearing near 2θ ≈ 35° and 57° can be assigned to iron oxide phases (Fe_2O_3/Fe_3O_4). The presence of these peaks confirms the successful loading of iron species onto the support. The relatively low intensity of the iron oxide peaks compared to copper peaks suggests that iron is more finely dispersed across the carbon surface, forming smaller crystallites or partially amorphous domains.The coexistence of amorphous carbon and crystalline metal oxide phases indicates the formation of a heterogeneous catalytic structure. The carbon support provides a high surface area for adsorption of azithromycin molecules, while the dispersed Cu and Fe oxides act as active catalytic centers for ozone activation and reactive oxygen species generation. The absence of large crystalline agglomerates further suggests that the impregnation and thermal treatment methods produced well-dispersed metal particles rather than bulk metal oxide phases. Therefore, the XRD results confirm that the Cu–Fe/activated carbon catalyst was successfully synthesized, and the presence of mixed copper and iron oxide phases is expected to enhance catalytic activity through redox cycling between Cu^{+}/Cu^{2+} and Fe^{2+}/Fe^{3+} species. These redox transitions facilitate ozone decomposition and hydroxyl radical formation, explaining the improved degradation efficiency of azithromycin observed in the electro-ozonation experiments.

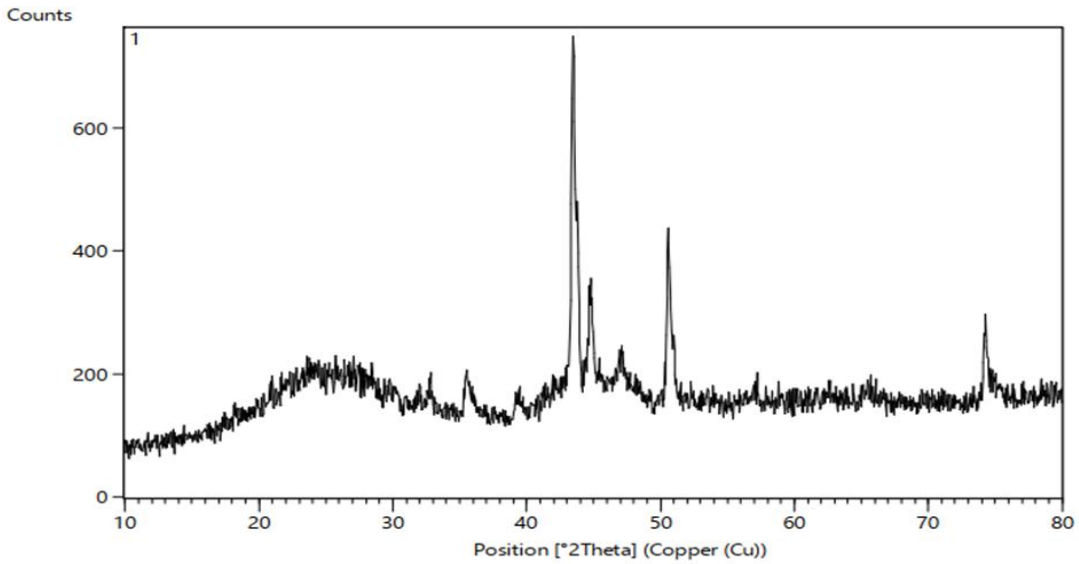

Figure (4): X-ray diffraction

3.2.3 FTIR

Fourier transform infrared spectroscopy (FTIR) **Figure (5)** was used to identify the surface functional groups of the Cu–Fe/activated carbon catalyst and to evaluate chemical interactions between the metal species and the carbon support. The FTIR spectrum shows several characteristic absorption bands corresponding to oxygen-containing functional groups on the activated carbon surface.A broad absorption band observed around 3414–3462 cm^{-1} is attributed to O–H stretching vibrations of surface hydroxyl groups and adsorbed water molecules. The presence of these hydroxyl groups is important because they act as anchoring sites for metal ions during the impregnation process and play a key role in catalytic ozonation reactions. The band at approximately 2897 cm^{-1} corresponds to aliphatic C–H stretching vibrations of residual organic structures within the carbon matrix. Peaks appearing at 1651–1622 cm^{-1} are assigned to C=O stretching and aromatic C=C skeletal vibrations of the graphitic carbon structure. These functional groups contribute to π–π interactions and adsorption of azithromycin molecules onto the catalyst surface. Additional bands located at 1541 and 1460 cm^{-1} are associated with aromatic ring vibrations and possible coordination interactions between metal ions and oxygen-containing groups on the carbon surface. The peak at 1396–1317 cm^{-1} can be attributed to C–O stretching vibrations of phenolic and carboxylic groups, indicating that the activated carbon contains abundant oxygenated functional groups. A strong absorption band observed near 1149–1045 cm^{-1} corresponds to C–O–C and C–O stretching vibrations of alcohol, ether, and ester groups. These groups are known to facilitate adsorption of pollutants and enhance electron transfer during catalytic reactions. In the lower wavenumber region (875–441 cm^{-1}), several new bands appear, which are characteristic of metal–oxygen (M–O) vibrations. These bands are attributed to Fe–O and Cu–O bonds, confirming the successful incorporation of iron and copper oxide species onto the activated carbon surface. The appearance of these metal–oxygen vibrations indicates that the metal ions are chemically bonded to the carbon support rather than physically adsorbed. The presence of hydroxyl groups together with Cu–O and Fe–O bonds suggests that the catalyst can promote redox cycling between Cu^{+}/Cu^{2+} and Fe^{2+}/Fe^{3+} species. These redox reactions facilitate ozone decomposition and hydroxyl radical generation. Therefore, the FTIR analysis confirms the formation of a chemically functionalized catalytic surface capable of enhancing reactive oxygen species production and improving azithromycin degradation in the electro-ozonation process.

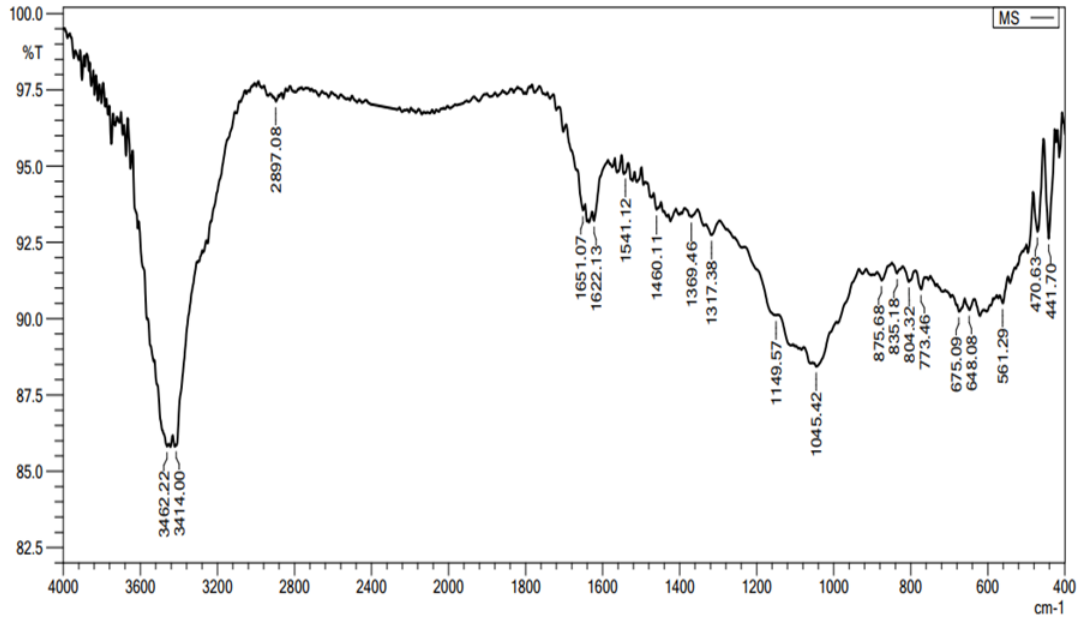

Figure (5): Fourier transform infrared spectroscopy

3.2.4 TGA Analysis

Thermo gravimetric analysis (TGA) **Figure (6)** was performed to evaluate the thermal stability and structural integrity of the synthesized Cu–Fe/activated carbon catalyst. The TG curve shows a very small total weight loss of approximately 1.34% over the entire temperature range up to about 900–1000 °C, indicating excellent thermal stability of the prepared catalyst. An initial minor weight loss observed below approximately 100 °C is attributed to the removal of physically adsorbed moisture and surface-bound water molecules trapped within the porous structure of the activated carbon. This behavior is typical for porous carbon materials due to their high surface area and hydrophilic oxygen-containing functional groups. Between 100 and 700 °C, the catalyst exhibited an almost constant mass with negligible decomposition. The absence of significant weight loss in this temperature region indicates that the carbon framework remained structurally stable and that most oxygen-containing surface functional groups were strongly bound to the carbon matrix. It also suggests that the impregnated Cu and Fe species were chemically anchored to the support and not present as loosely attached salts or unstable precursors. A slight mass decrease detected at temperatures above ~800 °C is associated with the slow thermal degradation of the carbon skeleton and partial oxidation of the carbonaceous structure. The limited weight loss at high temperature confirms that the majority of the catalyst consists of stable carbon and metal oxide phases. The extremely low overall weight change demonstrates that the impregnation and calcination procedures produced a robust catalyst with strong metal–support interactions. Such thermal stability is important for catalytic ozonation processes because it indicates resistance to structural collapse, metal leaching, and deactivation during electrochemical operation. Therefore, the TGA results confirm that the Cu–Fe/activated carbon catalyst possesses high thermal durability and structural stability, supporting its suitability for repeated electro-ozonation cycles and continuous wastewater treatment applications.

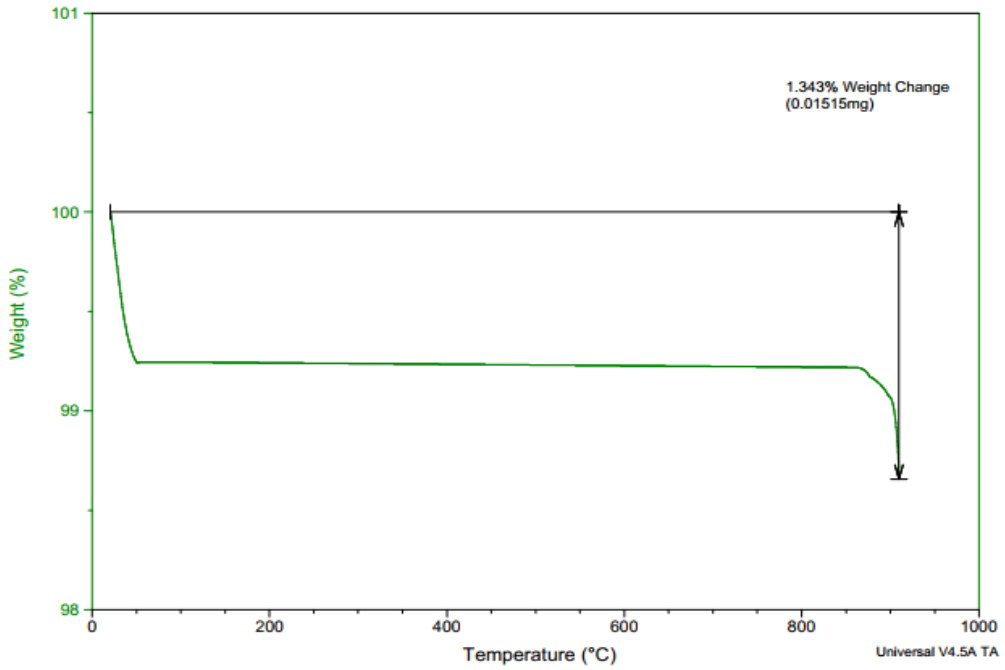

Figure (6): Thermo gravimetric analysis

3.2.5 SEM Analysis

Scanning electron microscopy (SEM) **Figure (7)** was used to examine the surface morphology and microstructure of the Cu–Fe/activated carbon catalyst at different magnifications. The low-magnification images reveal a highly porous carbon framework composed of irregular macrospores and interconnected cavities distributed throughout the structure. These cavities are characteristic of activated carbon and provide a large accessible surface area for pollutant adsorption and catalytic reactions. At intermediate magnification, the carbon surface appears covered with numerous granular deposits. These deposits are not part of the original carbon matrix and are attributed to the metal species introduced during the impregnation process. The particles are homogeneously distributed over the surface and along the pore walls, indicating effective penetration of the metal precursors into the porous structure rather than surface accumulation only. High-magnification SEM images show densely packed spherical and semi-spherical nanoparticles decorating the carbon surface. The measured particle sizes fall within approximately 50–65 nm, confirming the formation of nanoscale metal oxide clusters. The absence of large aggregates suggests good dispersion of Cu and Fe species and strong interaction with the carbon support. Furthermore, the nanoparticles are observed to anchor preferentially on defect sites and pore edges of the activated carbon. These locations correspond to high-energy sites where oxygen-containing functional groups are present, which is consistent with the FTIR results indicating surface hydroxyl and carboxyl groups. The deposition of metal oxides on these active sites promotes electron transfer and enhances catalytic activity. The porous structure remains intact after metal loading, indicating that the impregnation and thermal treatment did not collapse the carbon framework. Instead, the catalyst exhibits a hierarchical structure consisting of macrospores for mass transport and nanoscale particles providing catalytic active sites. Such architecture is highly beneficial for electro-ozonation processes because it facilitates diffusion of azithromycin molecules and ozone bubbles toward the active centers. Overall, SEM analysis confirms successful formation of a nanostructured heterogeneous catalyst with well-dispersed Cu–Fe particles anchored onto the activated carbon surface. The combination of high porosity and nanoscale metal dispersion explains the enhanced degradation efficiency observed in the electro-ozonation treatment of azithromycin.

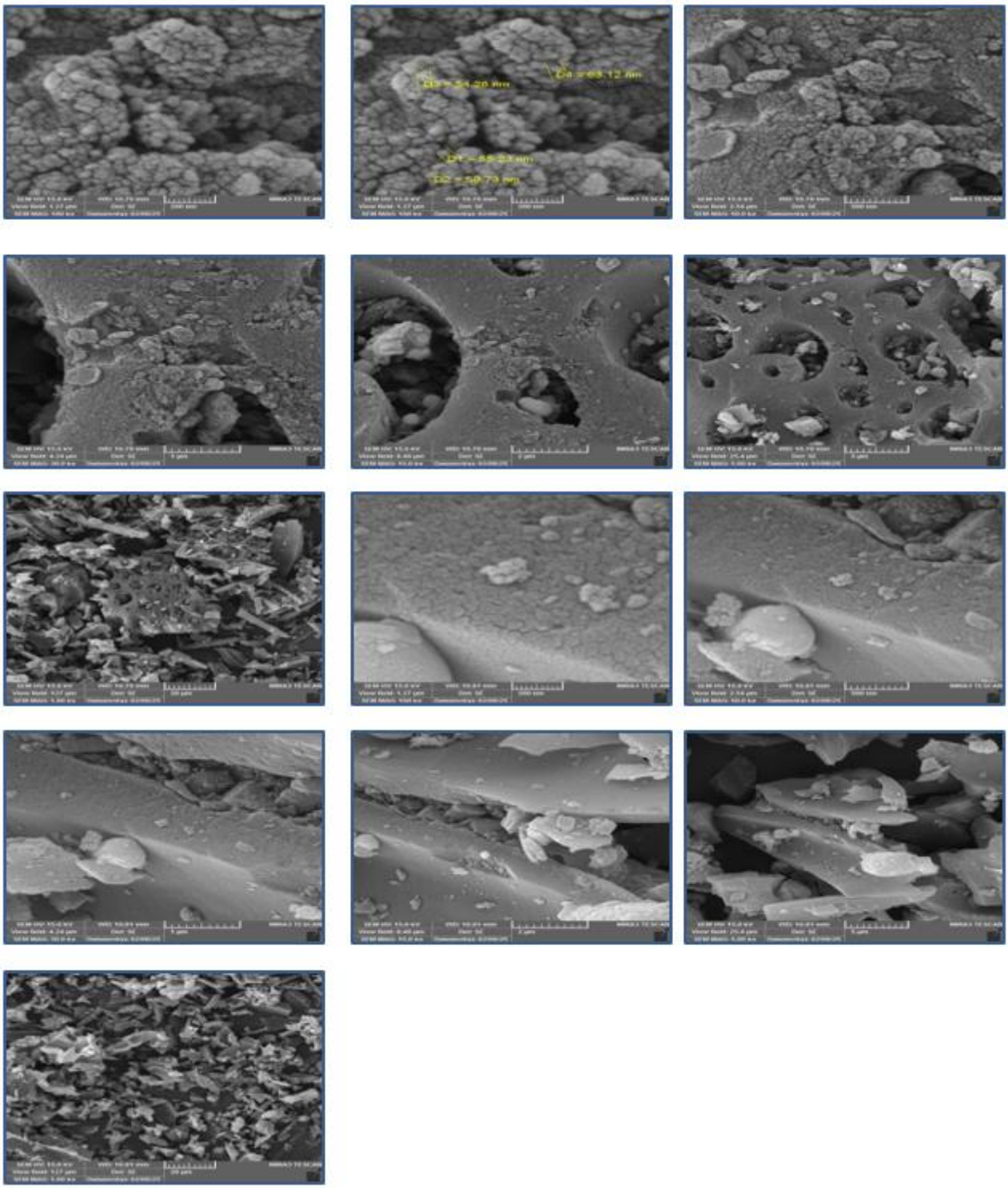

Figure (7): Scanning electron microscopy

3.2.6 BET analyses

The textural properties of the catalyst were tested by N 2 adsorption–desorption. The isotherm **Figure.(8)** of sample was characterized by rapid adsorption at low relative pressure and hysteresis-loops at higher pressure that correspond to a combined Type I/IV isotherm. This is indicative of the presence of both microspores and mesopores. A large specific

surface area of 740 $m^2 g^{-1}$ is calculated by BET adsorption, reflecting the porous nature of the material. From the pore size distribution **Figure(9),** most pores have a size between 2 and 5 nm. The microspores are the adsorption sites of azithromycin molecules, while the mesopores are the diffusion paths of ozone and reaction intermediates. The hierarchical porosity architecture favors the mass transfer, and promotes local concentration of pollutants around the catalytic sites, which enables direct oxidation reactions on catalyst surfaces rather than in the bulk solution

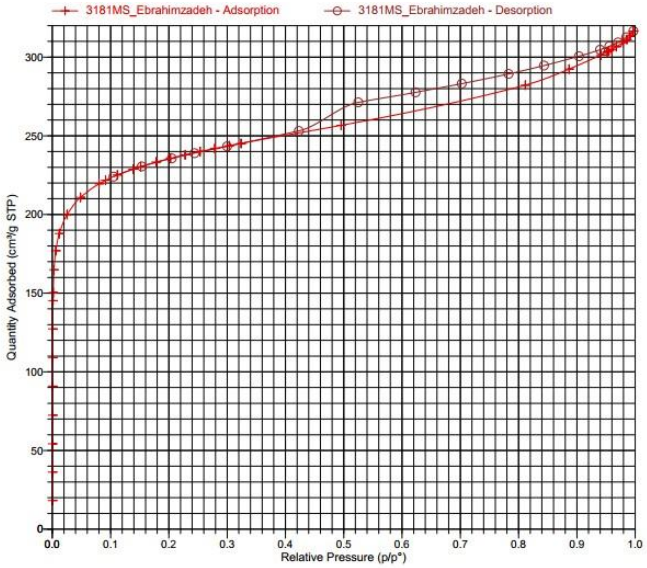

Figure (8): Brunauer-Emmett-Teller isotherm

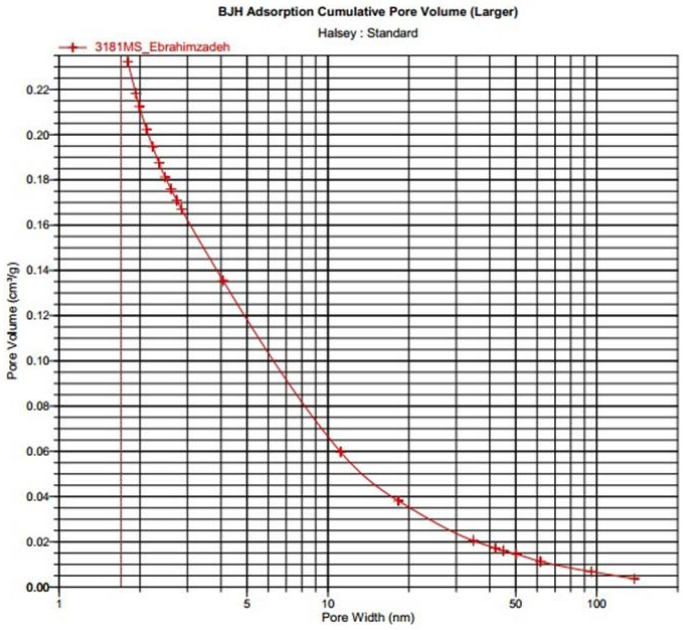

Figure (9): pore size distribution

3.2 Effect of hydrodynamic conditions: experimental trends and RSM validation

3.2.1 Influence of liquid flow rate and residence time

Experimental results revealed that AZM removal efficiency decreased with increasing liquid flow rate, indicating the critical role of hydraulic residence time in the continuous reactor. At lower flow rates, longer contact time facilitated effective interaction between AZM molecules, ozone bubbles, electrode surfaces, and catalytic sites, resulting in enhanced degradation.

In contrast, higher flow rates reduced contact time and limited pollutant–oxidant interactions**. Figure(10-14)**These experimental findings were strongly supported by Response Surface Methodology (RSM) analysis, which identified flow rate as one of the most statistically significant parameters influencing AZM conversion. The dominance of flow rate observed in RSM aligns well with the behavior of continuous advanced oxidation systems, where residence time governs reaction extent [21][11].

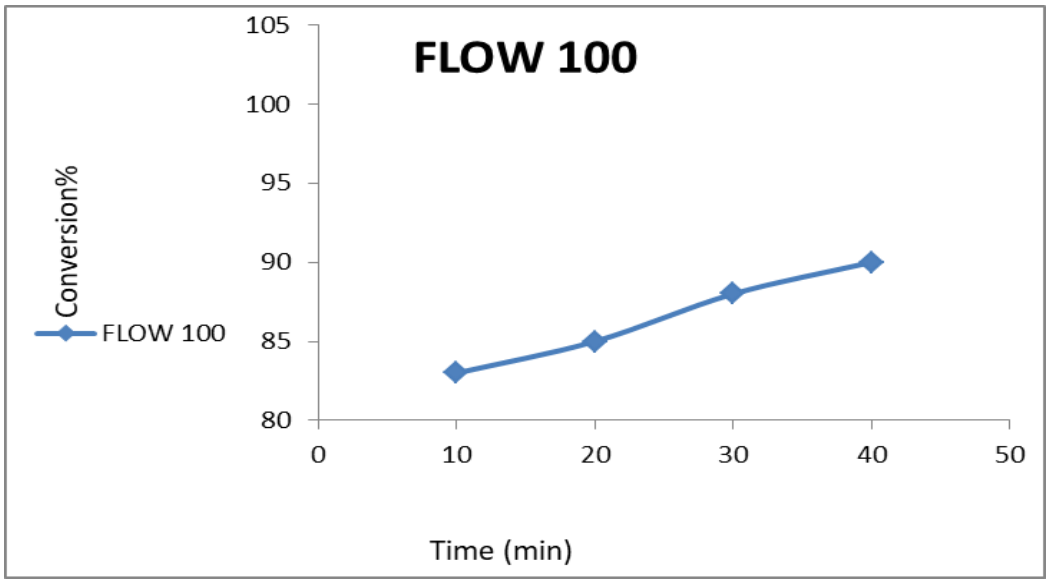

Figure (10)

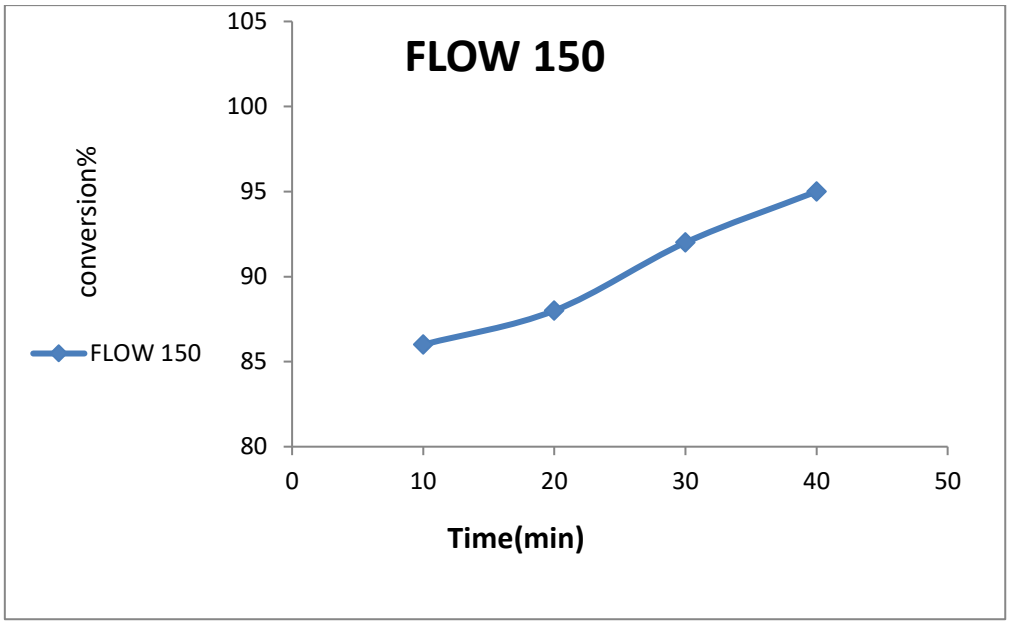

Figure (11)

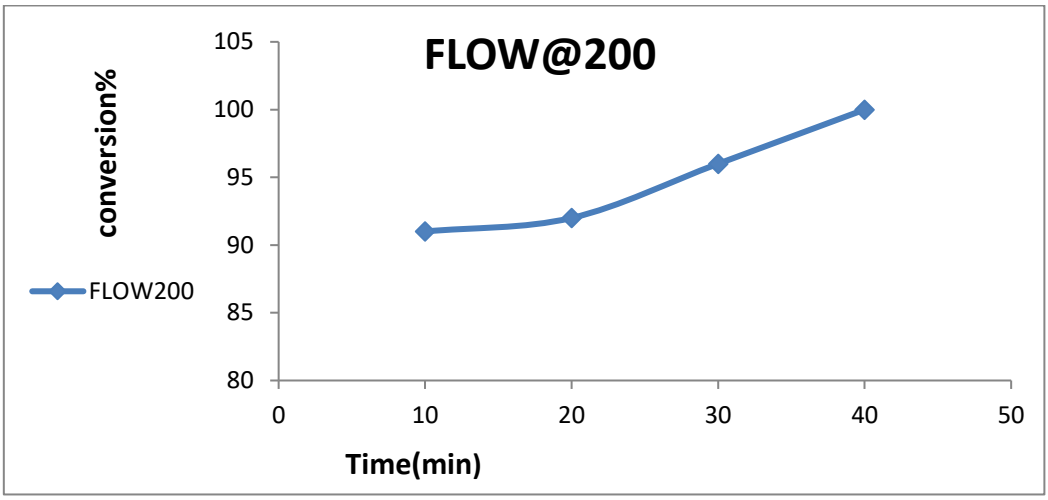

Figure (12)

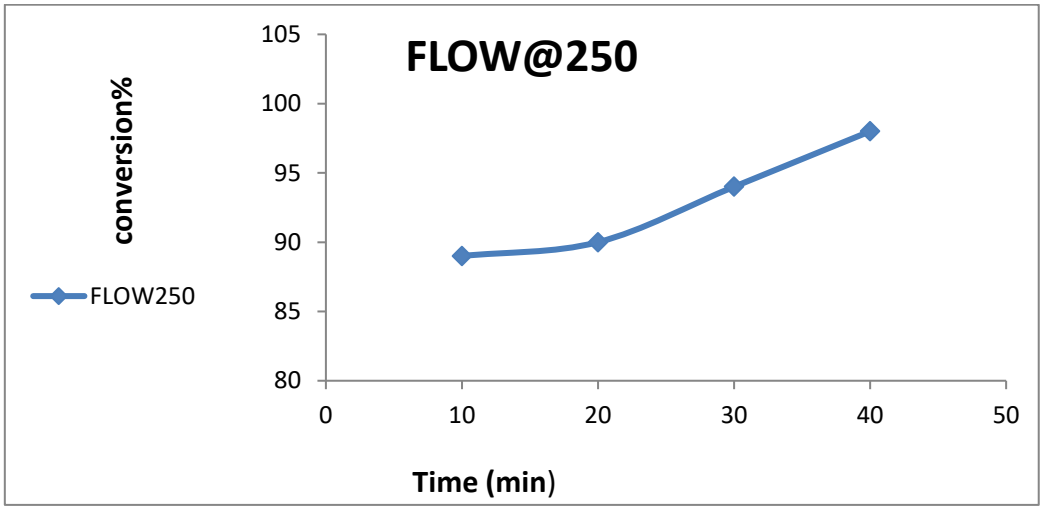

Figure (13)

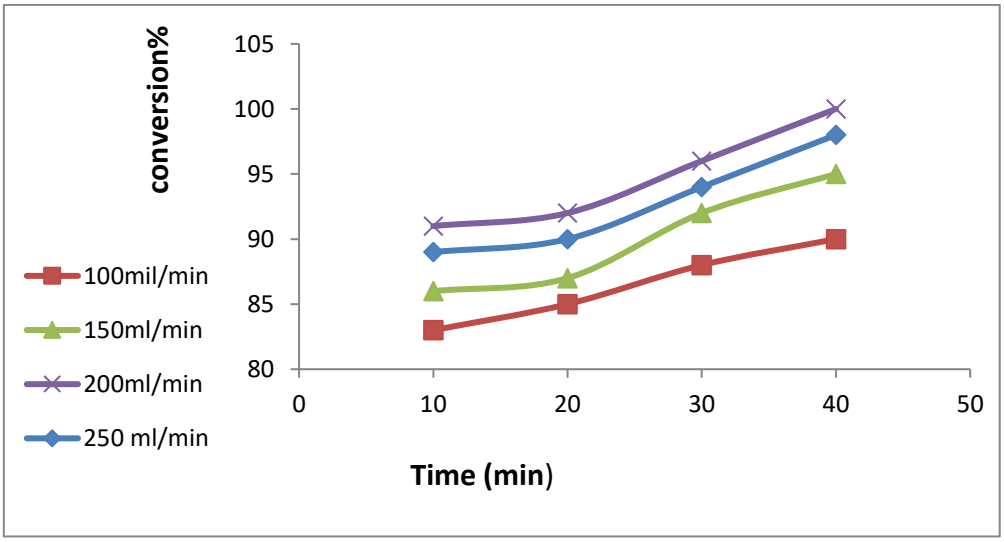

Figure (14)

3.2.2 Effect of reaction time and ozone flotation

The AZM degradation was enhanced by increasing ozone sparing rate, and the increase in gas–liquid mass transfer and additional available ozone were important factors to improve the reaction because of it. However, the performance was to a certain extent improved when further increasing ozone flow rate higher than an optimum value. Then, the results revealed that some portion of ozone was wasted and used inefficiently. The similar phenomenon was reported in ozonation catalytic [9] and electro-ozonation treatment of pharmaceutical pollutants [9].Statistical analysis (RSM) confirmed that the reaction time was also a significant factor, highlighting the requirement of an adequate exposure to oxidizing species. The good agreement between experimental data and statistical predications indicate that the RSM model can reasonably explain the influencing factors in operation

3.2.3 ANOVA interpretation paragraph (INSERT-READ)

The validity of the established RSM model was confirmed according to the analysis of variance (ANOVA) Table(1). The model had a rather high F and probability value ($p < 0.0001$), which meant that the regression model was highly significant, with the effect of azithromycin conversion was not due to random experimental error. The great value of the coefficient of determination (R^2) and by fitting agreement among R^2 adjusted and predicted confirmed that such reliability and power to predict these values in relation the model. Liquid flow rate and reaction time were determined to be statistically significant parameters for azithromycin removal from the factors studied, while concentration of electrolyte, initial concentrations and temperature showed relatively smaller effects within the range investigated. Residuals Residuals were found to be clustered near a zero line on normal probability plots and an approximately 1 stochastic scatter pattern was attained. Responses, confirming that the model adequately described the experimental data and could be used for process optimization. Factor coding is Coded. Sum of squares is Type III – Partial The Model F-value of 1072.58 implies the model is significant. There is only a 0.01% chance that an F-value this large could occur due to noise-values less than 0.0500 indicate model terms are significant. In this case A, D are significant model terms. Values greater than 0.1000 indicate the model terms are not significant. If there are many insignificant model terms (not counting those required to support hierarchy), model reduction may improve your mod

3.3 Effect of pH and temperature

Factors that affect pH, such as the type of catalyst used and salt content, strongly influenced AZM degradations behaviors apparently due to its influence on ozone stability, radical generation in solution and surface charge of the catalyst. Experimental results provided that both neutral and moderately alkaline ranges promoted AZM degradation, implying the presence of direct ozone interference and radical induced reactions. A similar pH-sensitive manner has been documented for the catalytic ozonation of antibiotics [9].The decomposition of AZM enhanced when temperature rose from 25 to 50 °C, implied that the oxidation process was thermally induced. Higher temperatures are increasing the rate of ozone decomposition and reaction kinetics, which will create more ROS Figure (15). First-order kinetics kinetic studies revealed that the degradation of AZM followed a pseudo-first order model, which was similar to the previous EO [14], [10] While temperature was found to be non-significant in the RSM model over the range studied this is not inconsistent with observation, but rather implies that hydrodynamic parameters play a greater role within our chosen operating space, as is often found for multivariate screening studies [21].

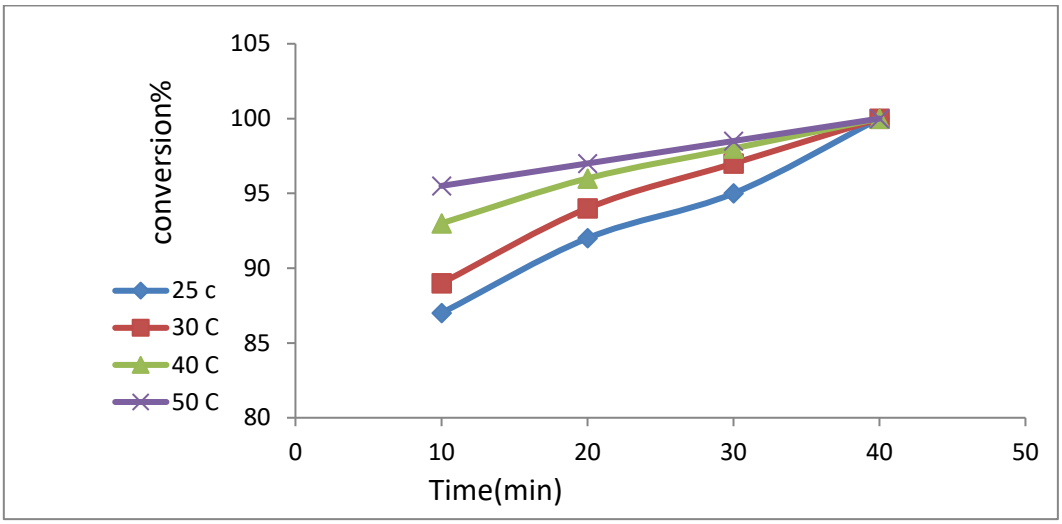

Figure (15)

3.4 Experimental design and statistical Analysis of variance (ANOVA)

An experimental design was applied by varying operational parameters to evaluate the azithromycin (AZI) removal from aqueous solutions and analysis of variance (ANOVA). The independent factors were the flow rate (A), type of electrolyte (B), initial AZI concentration (C), reaction time (D) and temperature (E), while azithromycin removal percentage was the response variable. Statistical replicates were performed for each experimental condition.in design expert software (v.13) table (1)

The overall model was statistically significant ($F = 97.80$, $p < 0.0001$) via analysis of variance (ANOVA), suggesting that the factors and interactions selected adequately explained the variation in AZI removal efficiency. Both the flow rate (A, $F = 515.06$, $p < 0.0001$) and reaction time (D, $F = 672.74$, $p < 0.0001$), among primary parameters had highly significant effects while as electrolyte type (B, $F = 4.48\times10\text{-}13$, $p = 1.0000$), initial AZI concentration (C, $F=2.24\times10\text{-}13$,$p\simeq1.0000$) and temperature (E,$F=1.12\times10\text{-}13$,$p\simeq1.0000$) showed no significant influence on removal efficiency

Interactions of significance were also observed. In particular, the AB and AC interactions ($F = 7.81$, $p = 0.0070$), and AD ($F = 27.15$, $p < 0.0001$), AE ($F =51\cdot85$, P\textless0·0001) were all significant contributors of variability in AZI removal represented by aleatory interaction factors BC ($F =83\ 06\ p < 0\cdot0001$). Residual error was low (Residual MS = 0.2537), indicating strong fit of the model. The fit was good (Lack of Fit MS = 7.48).

Conclusion: The factorial design with ANOVA not only identified the most important factors and interactions influencing azithromycin removal but also provided quantitative basis for optimizing process conditions. The importance of flow rate and reaction time, plus some interactions between other factors play an essential role for achieving the maximum removal efficiency as demonstrated by these results.

Table (1) analyses of variance (ANOVA)

Source	Sum of Squares	df	Mean Square	F-value	p-value	Remark
Model	248.12	10	24.81	97.8	< 0.0001	significant
A-flow	130.67	1	130.67	515.06	< 0.0001	
B-Electrolyte	1.14E-13	1	1.14E-13	4.48E-13	1	

C-initial conc.of AZI (ppm)	5.68E-14	1	5.68E-14	2.24E-13	1	
D-Time	170.67	1	170.67	672.74	< 0.0001	
E-temprture	2.84E-14	1	2.84E-14	1.12E-13	1	
AB	1.98	1	1.98	7.81	0.007	
AC	1.98	1	1.98	7.81	0.007	
AD	6.89	1	6.89	27.15	< 0.0001	
AE	13.15	1	13.15	51.85	< 0.0001	
BC	21.07	1	21.07	83.06	< 0.0001	
Residual	14.97	59	0.2537			
Lack of Fit	14.97	2	7.48			
Pure Error	0	57	0			
Cor Total	263.09	69				

3.5.1 Fit Statistic Analysis of Variance

The adequacy and predictive capability of the experimental azithromycin removal model received a fit statistics assessment. The residuals showed low standard deviation (Std. Dev. = 0.2091), implying a minor divergence of the experimental values from model predictions. The overall mean was 88.31% performance of the treatment process indicating the removal efficient through all runs. The model's quality and predictive capability are summarized in **Table 2**The coefficient of determination was also high (R^2 = 0.9884), which means that the model factors explained nearly all variability in azithromycin removal, at 98.84%. The adjusted R^2 (0.9871) affirmed the model robustness, even with accounting for the number of predictors, and the predicted R^2 (0.8836) illustrated strong predictive performance against new experimental conditions. The coefficient of variation (C.V. % = 0.237%) was very low, indicative of the reproducibility and precision of these experiments. In addition, the adequate precision value (200.08) was much higher than the desired threshold of 4, also confirming a encouraging signal to noise ratio and that this model could reliably be used to search the design space. In summary, these fit statistics suggest that a very good quality and reproducible predictive model has been developed to provide the well-founded quantitative basis for optimizing operational parameters in azithromycin removal experiments. Model accuracy within the design space is also illustrated in the additional response surface and contour plots (Figures 16) The majority of the design points, shown in the contour plot with areas of low standard error (which are around 0.01–0.2) within the center of the design space show reliable predictions from the models within this region. These findings are further illustrated in the 3D surface plot, which indicates that the standard error tends to increase toward the edges of the boundary (as more expected for RSM). These graphical analyses present a clear visualization of the best area to choose operating parameters in order to maximize AZI removal.

Table (2) Fit Statistics

Std. Dev.	0.2091	**R^2**	0.9884
Mean	88.31	**Adjusted R^2**	0.9871
C.V. %	0.2367	**Predicted R^2**	0.8836
		Adeq Precision	200.0781

Natural Resources for Human Health
eISSN: 2583-1194

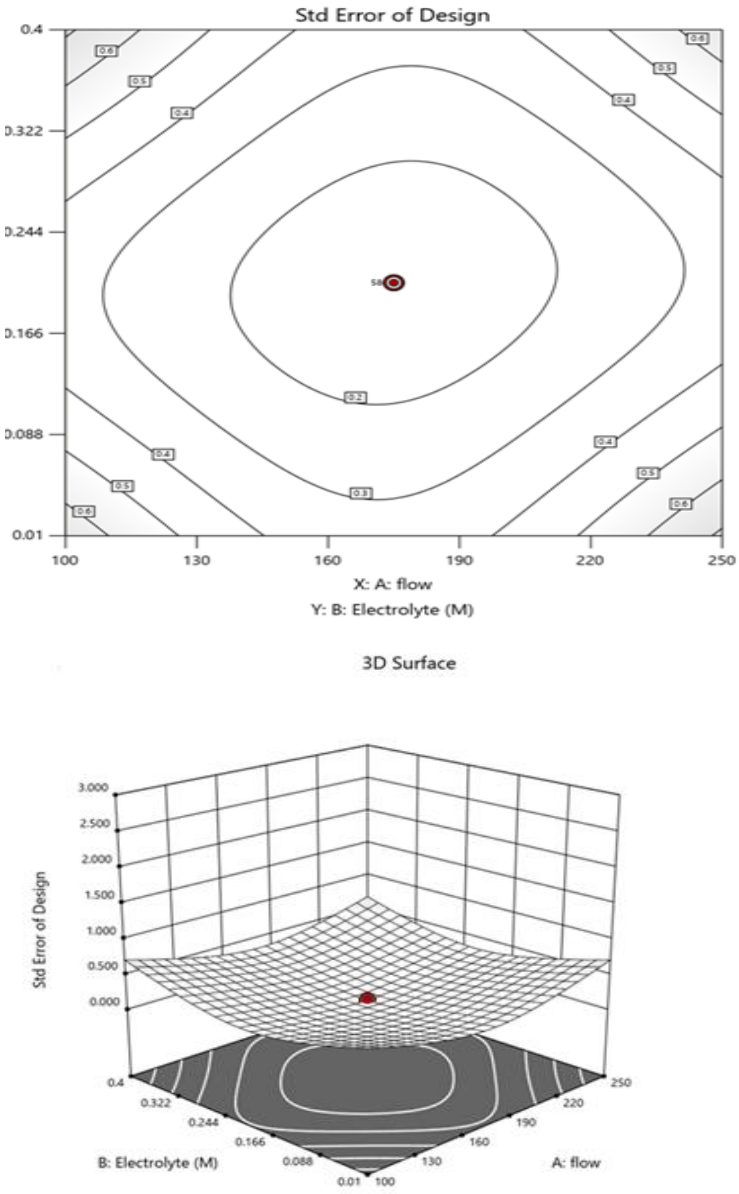

Figure (16) Contour and 3D surface plots of the standard error of design

3.5.2 *Diagnostics for ODS Model*

Model verification was also performed using diagnostic plots to check the assumptions of ordinary least squares (OLS) and response surface methodology for azithromycin removal. The residuals vs. run plot **Figure (17)** shows that the residuals are scattered randomly around zero meaning there are no unaccounted systematic errors or trends over regards experimental runs. The Durbin–Watson statistic of 3.0417 confirms that there is no positive autocorrelation in residuals while the randomness factor (−0.5417) still lies within permissible limits, validating independence assumption. The normal probability plot of residuals **Figure(18)** confirms that the residuals closely follow a straight line and thus, the errors are approximately normally distributed. And this fulfills the normality assumption of the independent error term (which is also needed for reliable ANOVA and regression inference). A residuals vs. predicted values plot **Figure(19)** confirms that the model captures the response behavior over the range studied, with a random scatter around zero with no apparent patterns emerging. Finally, the predicted vs actual plot **in Fig.(20)** shows that the predicted values to flow conversion fit well with measured data points and explains very good model predictability and bias free output.These individual diagnostics together

confirm the statistical adequacy of the ODS model, where there were no obvious violations of independence, normality and constant variance which contribute towards reliable predictions that aid in maximizing removal of azithromycin as our objective.

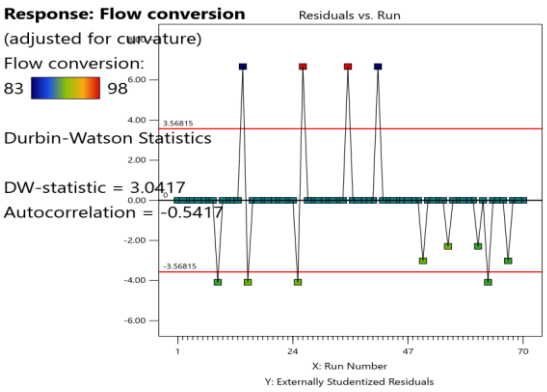

Figure (17): The residuals vs. run plot

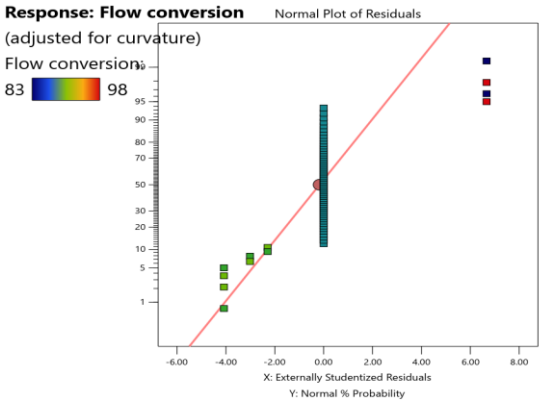

Figure(18): The normal probability plot of residuals

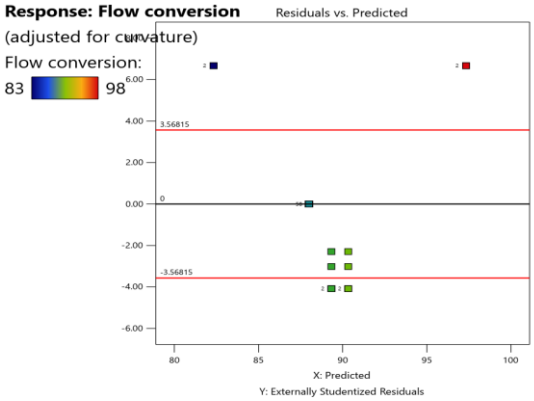

Figure (19): A residuals vs. predicted values plot

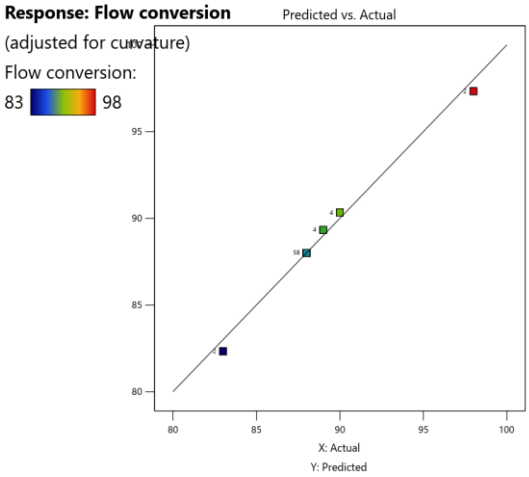

Figure(20): the predicted vs. actual plot

3.5.3. The Effect of ODS Variables azithromycin

The effect of five operating variables on azithromycin removal by ODS was studied through a fitted quadratic model. Thus the last empirical coded factors equation was: (A: flow rate; B: electrolyte concentration; C: AZI initial concentration; D: reaction time and E: temperature.)

Flow Conversion (%)= 89.83+3.50A+0.0000B+0.0000C+4.00D+0.0000E+0

Both flow rate (A) and reaction time (D) significantly showed positive effects on the azithromycin removal, as confirmed by the model coefficients and ANOVA analysis, whereas electrolyte concentration (B), initial AZI concentration (C), temperature (E) and the two-factor interaction AB were not significant at $p > 0.65$. This represents that, within the studied range, the removal efficiency increased as flow rate and reaction time raised but did not significantly affected by electrolyte concentration, initial AZI concentration, temperature and their interaction. A 3D response surface plot and associated contour plot replicate the synergistic impact of flow rate and electrolyte concentration influences on azithromycin removal at mid-range levels of the other parameters (C = 32.5 ppm, D = 25 min, E = 42.5 °C). Across the design space, a higher flow conversion occurs at advancing flow rate meaning this is strictly monotonic and is found from both the 3D surface plot and contour as shown in **Figure(20)**. Supplemental contour plot **Figure (21)** includes the fact that electrolyte concentration has only a minor impact here, as vertical contour lines confirm! DescriptionReasonIt is NOT clear we used main-effects plots see **figure (22)** which clearly shows the individual effect of each factor. The flow rate (A) and reaction time (D) also show a clear

positive slope, indicating their strong contribution to improving azithromycin removal as well. Conversely, the electrolyte concentration (B), initial AZI concentration (C), and temperature (E) are almost horizontal, showing little effect change in the range used in this study. The plot of interaction for AB is also flat, and thus supports the absence of interaction between these two factors in AP. ConclusionsUnder the experimental conditions applied in this study, only maximum flow rate and reaction time increase azithromycin removal by ODS, while electrolyte concentration, initial AZI concentration, temperature and their interaction do not exert an influence in the tested ranges. These visual displays unequivocally map the effect of operational parameters on removal efficiency and formulate a quantitative and graphical basis for enhancing the proces

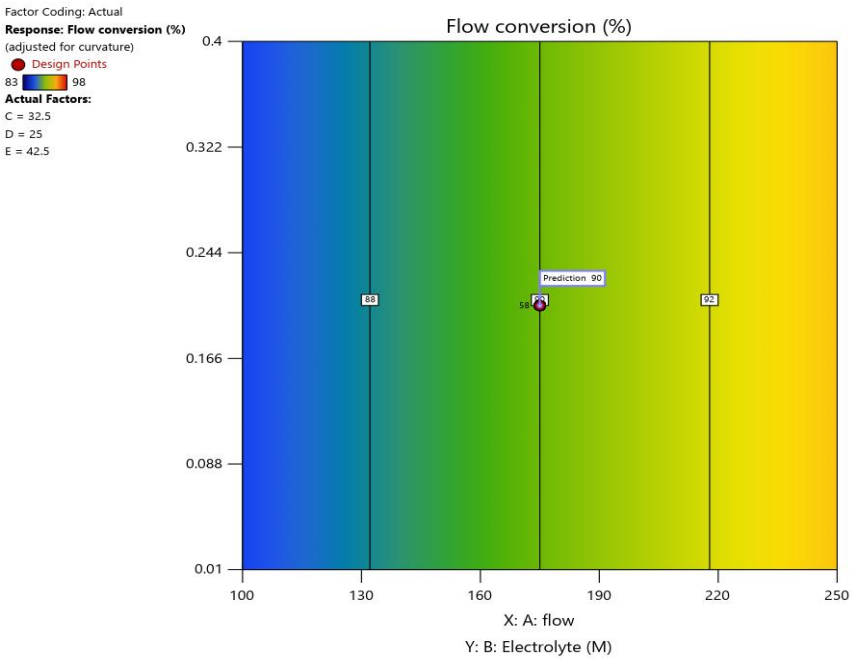

Figure (20) : surface plot showing the effect of flow rate and electrolyte concentration on azithromycin removal

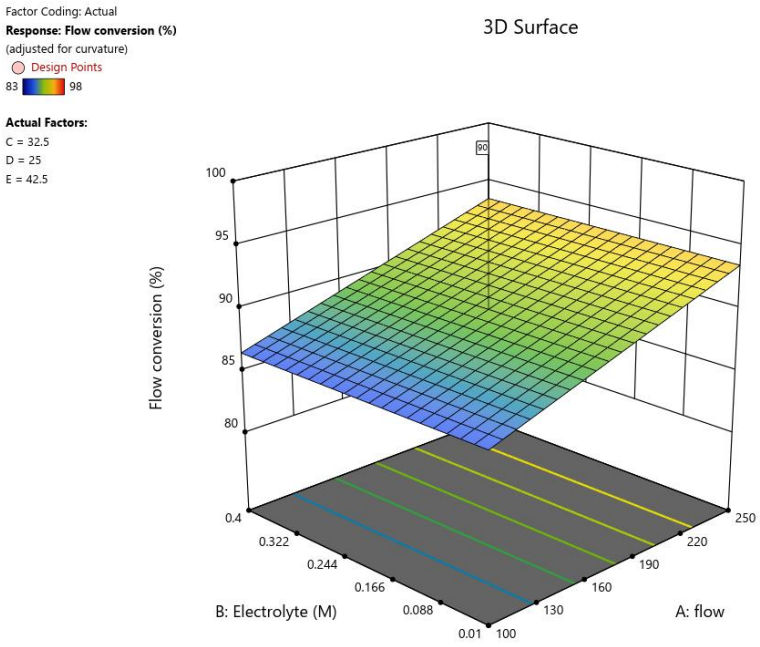

Figure (21): Contour plot of flow conversion illustrating minimal influence of electrolyte concentration

Natural Resources for Human Health
eISSN: 2583-1194

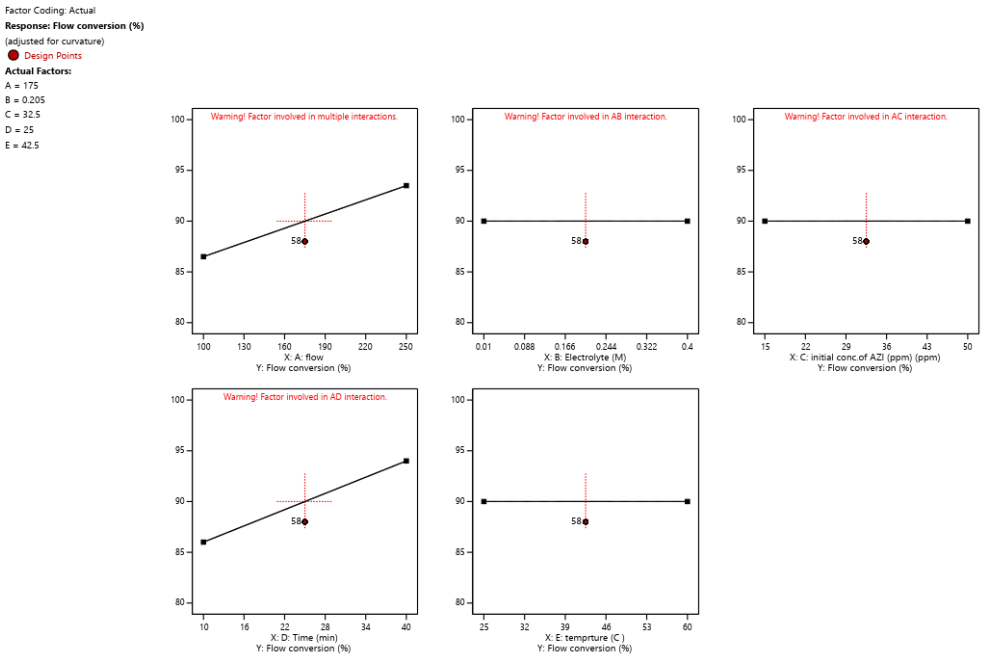

Figure (22): Main-effects and interaction plots of all factors (A–E) showing the dominant effect of flow rate and reaction time

3.5.4. Numerical Optimization of removal azithromycin

To define the favorable operational conditions to maximize azithromycin (AZI) removal by ODS, numerical optimization was performed in **Design-Expert® Version 13 (Stat-Ease Inc).** Finally, the flow conversion predicted by the fitted quadratic model across the entire design space was evaluated as a function of flow rate (A), electrolyte concentration (B), initial AZI concentration (C), reaction time (D), and temperature (E).**Figure (23)** 3D surface plot shows that the flow rate greatly improves the AZI removal meanwhile, there is little influence of electrolyte concentration. The respective contour plot **Figure (24)** identifies the desirable design region, which demonstrates solid flow conversion (~90 %) at high flow rates and intermediate levels of each other factors (C = 32.5 ppm, D = 25 min, E = 42.5 °C).The numerical optimization results show that the dominant factors influencing AZI removal efficiency are flow rate and reaction time, while variation in electrolyte concentration, initial AZI concentration and temperature have relatively minor influences. The removal was predicted to increase from around 84.5% for the lowest flow rate (100 L h^{-1}) up to approximately 94% for the highest flow rate (250 L h^{-1}), showing a monotonic, progressive improvement in response. The contour map provides additional evidence that electrolyte concentration has a negligible effect due to nearly vertical contour lines confirming model robustness.These results indicate that maximizing the flow rate and reaction time is sufficient to achieve high removal efficiency, thereby providing clear guidance for the practical application of ODS for AZI removal**. Design-Expert 13** employed for accurate numerical optimization and graphical visualization all over the design space that makes process optimization efficient.

Natural Resources for Human Health
eISSN: 2583-1194

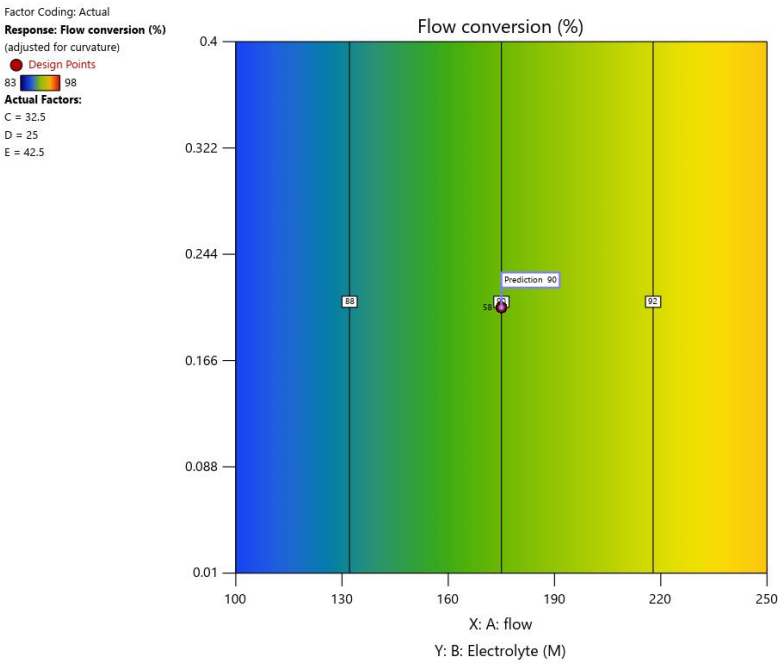

Figure(23): 3D surface plot showing the influence of flow rate and electrolyte concentration on azithromycin removal

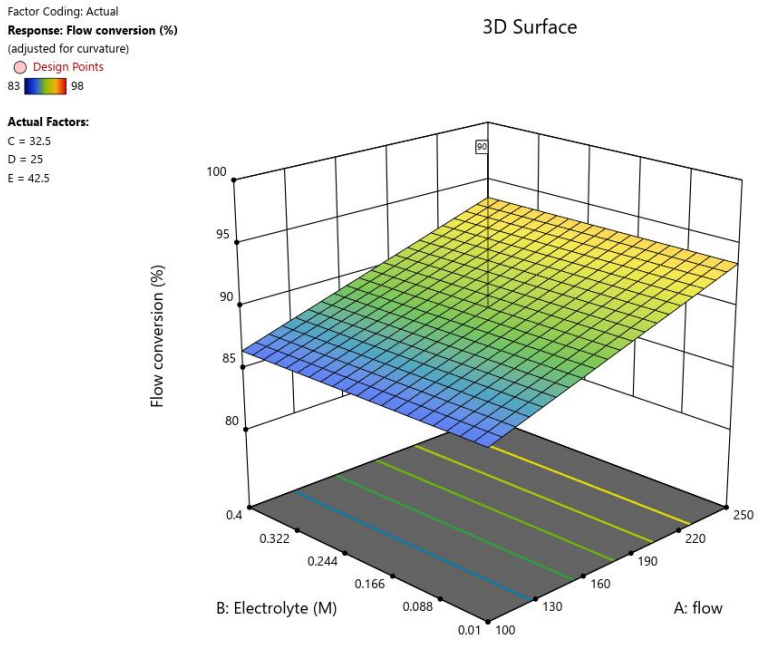

Figure(24): Contour plot highlighting the optimal region for maximal AZI removal

4. CONCLUSIONS

A Cu(5%)–Fe(5%)/activated carbon catalyst was successfully prepared and employed for the degradation of azithromycin in water through a combined approach of electro-oxidation with ozonation (EO/O3). The integrated process exhibited much higher degradation efficiency than single ozonation and electrochemical oxidation, proving synergistic effect of electrochemical activation, catalytic ozone and adsorption. The formation of the heterogeneous catalytic structure was skin

deep supported by a complete physicochemical characterization. The highly porous and rough surface, which was also decorated with well-dispersed nanoparticles (~50–65 nm) across the SS material with many accessible active sites, were confirmed by SEM and AFM images. XRD revealed the crystalline phases of copper and iron oxides were attached on an amorphous carbon matrix, whereas FTIR showed the formation of metal-oxygen bonds and surface oxygen-containing functional groups associated with pollutant capture and metal immobilization. Evaluation through BET analysis showed a high specific surface area and hierarchical micro–mesoporous properties which facilitated the mass transfer and absorption of azithromycin molecules near catalytic sites. TGA data also demonstrated good thermal and structural stability, confirming the presence of strong metal–support interactions and protection against catalyst poisoning .Experimental studies and statistical model indicated that hydrodynamic parameters such as the liquid flow rate and the reaction time largely controlled the degradation process. The high model significance by ANOVA and the strong predictive ability of the RSM model indicated that in the studied system's operating range, performance is mainly dictated by residence time and mass transfer rather than temperature influence. The degradation pathway is proposed involving an adsorption–catalytic oxidation scheme, where azithromycin molecules are adsorbed on high-surface-area carbon support, then catalytically oxidized by activated ozone at Cu and Fe redox centers (Cu^{+}/Cu^{2+} and Fe^{2+}/Fe^{3+}) leading to the formation of reactive oxygen species, predominantly hydroxyl radical. The good contact of adsorbed pollutants with in situ produced oxidants accounts for the improvement removal efficiency of EO. In conclusion, the prepared catalyst possesses an excellent stability, fine dispersion of active phases and good catalytic performance under a low applied voltage operation, which shows the promising application potential in continuous wastewater treatment. The results indicate that amalgamating ozonation/catalytic oxidation and adsorption in a reactor is an efficient concept to remove antibiotic pollutants and provide a feasible approach for the development of novel hybrid oxidation systems for non-persistent/toxic emerging contaminants.

REFERENCES

[1] C. Peña-Guzmán *et al.*, "Emerging pollutants in the urban water cycle in Latin America: A review of the current literature," *J. Environ. Manage.*, vol. 237, pp. 408–423, 2019, doi: https://doi.org/10.1016/j.jenvman.2019.02.100.

[2] E. Lampi, F. Carlsson, G. Jacobsson, T. Sterner, and D. G. J. Larsson, "Willingness to pay for antibiotic pollution control," *Ecol. Econ.*, vol. 239, p. 108780, 2026, doi: https://doi.org/10.1016/j.ecolecon.2025.108780.

[3] A. Mehrdoost, R. Jalilzadeh Yengejeh, M. K. Mohammadi, A. A. Babaei, and A. Haghighatzadeh, "Comparative Analysis of UV-assisted Removal of Azithromycin and Cefixime from Aqueous Solution Using PAC/Fe/Si/Zn Nanocomposite," *J. Heal. Sci. Surveill. Syst.*, vol. 9, no. 1, pp. 39–49, 2021, doi: 10.30476/jhsss.2020.88564.1149.

[4] P. A. Cano, M. Jaramillo-Baquero, H. Zúñiga-Benítez, Y. A. Londoño, and G. A. Peñuela, "Use of simulated sunlight radiation and hydrogen peroxide in azithromycin removal from aqueous solutions: Optimization & mineralization analysis," *Emerg. Contam.*, vol. 6, pp. 53–61, 2020, doi: https://doi.org/10.1016/j.emcon.2019.12.004.

[5] R. Jalilzadeh, R. Shokri, A. Almasi, and A. Babaei, "Advanced Oxidation Process Efficiently Removes Ampicillin from Aqueous Solutions," *Iran. J. Toxicol.*, vol. 14, pp. 123–132, Apr. 2020, doi: 10.32598/ijt.14.2.483.3.

[6] L. A. Bermúdez, J. M. Pascual, M. D. Martínez, and J. M. Poyatos Capilla, "Effectiveness of Advanced Oxidation Processes in Wastewater Treatment: State of the Art," 2021. doi: 10.3390/w13152094.

[7] F. Mirzaie *et al.*, "Occurrence and distribution of azithromycin in wastewater treatment plants, seawater, and sediments of the northern part of the Persian Gulf around Bushehr port: A comparison with Pre-COVID 19 pandemic," *Chemosphere*, vol. 307, p. 135996, 2022.

[8] A. Giwa *et al.*, "Recent advances in advanced oxidation processes for removal of contaminants from water: A comprehensive review," *Process Saf. Environ. Prot.*, vol. 146, pp. 220–256, 2021, doi: https://doi.org/10.1016/j.psep.2020.08.015.

[9] J. Wang and H. Chen, "Catalytic ozonation for water and wastewater treatment: Recent advances and perspective," *Sci. Total Environ.*, vol. 704, p. 135249, 2020, doi: https://doi.org/10.1016/j.scitotenv.2019.135249.

[10] N. N. Roslan *et al.*, "Recent Advances in Advanced Oxidation Processes for Degrading Pharmaceuticals in Wastewater—A Review," 2024. doi: 10.3390/catal14030189.

[11] J. Mukherjee *et al.*, "Advanced oxidation process for the treatment of industrial wastewater: A review on strategies, mechanisms, bottlenecks and prospects," *Chemosphere*, vol. 345, p. 140473, 2023, doi: https://doi.org/10.1016/j.chemosphere.2023.140473.

[12] P. Leinweber, J. Malý, and T. Weidlich, "Carbon-Based Catalysts in Ozonation of Aqueous Organic Pollutants," *Catalysts*, vol. 16, p. 41, Jan. 2026, doi: 10.3390/catal16010041.

[13] Z. Shahbeiki, M. Khodadadi, Y. Dadban-Shahamat, and H. Nadimi, *Integrated Persulfate/Ozonation Process Using Fe_3O_4/AC Catalyst for Antibiotic Degradation: Optimization and Kinetic Insights*. 2025. doi: 10.21203/rs.3.rs-7696908/v1.

[14] Y. Ling *et al.*, "Efficient photocatalytic ozonation of azithromycin by three-dimensional g-C3N4 nanosheet loaded magnetic Fe-MCM-48 under simulated solar light," *Appl. Catal. B Environ.*, vol. 324, p. 122208, 2023, doi: https://doi.org/10.1016/j.apcatb.2022.122208.

[15] C. C. Castro-Jiménez, J. C. Saldarriaga-Molina, E. F. García, R. A. Torres-Palma, and N. Acelas, "Azithromycin removal from water via adsorption on drinking water sludge-derived materials: Kinetics and isotherms studies," *PLoS One*, vol. 20, no. 1, p. e0316487, Jan. 2025, [Online]. Available: https://doi.org/10.1371/journal.pone.0316487

[16] M. Dana, M. A. Sobati, S. Shahhosseini, and A. Ansari, "Optimization of a continuous ultrasound assisted oxidative desulfurization (UAOD) process of diesel using response surface methodology (RSM) considering operating cost," *Chinese J. Chem. Eng.*, vol. 28, no. 5, pp. 1384–1396, 2020, doi: https://doi.org/10.1016/j.cjche.2019.12.007.

[17] M.-C. Lu, L. Biel, M.-W. Wan, R. de Leon, and S. Arco, "The Oxidative Desulfurization of Fuels with a Transition Metal Catalyst: A Comparative Assessment of Different Mixing Techniques," *Int. J. Green Energy*, vol. 11, pp. 833–848, Jan. 2014, doi: 10.1080/15435075.2013.830260.

[18] E. Karami, M. A. Sobati, B. Khodaei, and K. Abdi, "An experimental investigation on the ultrasound-assisted oxidation of benzothiophene in model fuel: Application of response surface methodology," *Appl. Therm. Eng.*, vol. 118, pp. 691–702, 2017, doi: https://doi.org/10.1016/j.applthermaleng.2017.03.028.

[19] A. Rasmuson, B. Andersson, L. Olsson, and R. Andersson, *Mathematical Modeling in Chemical Engineering*. Cambridge: Cambridge University Press, 2014. doi: DOI: 10.1017/CBO9781107279124.

[20] K. Hinkelmann, *Design and Analysis of Experiments*. 2012. doi: 10.1002/9781118147634.

[21] D. Montgomery and C. St, *Design and Analysis of Experiments, 9th Edition*. 2022.